Journal of Biomolecular NMR, **25:** 281–290, 2003.
KLUWER/ESCOM

Chemical shift-dependent apparent scalar couplings: An alternative concept of chemical shift monitoring in multi-dimensional NMR experiments

Witek Kwiatkowski & Roland Riek*
Structural Biology Laboratory, The Salk Institute, La Jolla, CA 92037, U.S.A.

Received 11 September 2002; Accepted 16 December 2002

Key words: biological macromolecule, chemical shift, chemical shift-coded experiment, multi-dimensional experiment, NMR, triple resonance experiment

Abstract

The paper presents an alternative technique for chemical shift monitoring in a multi-dimensional NMR experiment. The monitored chemical shift is coded in the line-shape of a cross-peak through an apparent residual scalar coupling active during an established evolution period or acquisition. The size of the apparent scalar coupling is manipulated with an off-resonance radio-frequency pulse in order to correlate the size of the coupling with the position of the additional chemical shift. The strength of this concept is that chemical shift information is added without an additional evolution period and accompanying polarization transfer periods. This concept was incorporated into the three-dimensional triple-resonance experiment HNCA, adding the information of $^{1}H^{\alpha}$ chemical shifts. The experiment is called HNCA^{coded}HA, since the chemical shift of $^{1}H^{\alpha}$ is coded in the line-shape of the cross-peak along the $^{13}C^{\alpha}$ dimension.

Abbreviations: HNCA – amide proton-to-nitrogen-to-alpha-carbon correlation; HNCA^{coded}HA – HNCA with the additional frequency of alpha-hydrogens coded in the multiplet pattern of the cross-peaks along the alpha-carbon frequency; INEPT – insensitive nuclei enhanced by polarization transfer; NMR – nuclear magnetic resonance; PFG – pulsed field gradient; TROSY – transverse relaxation-optimized spectroscopy; 2D, 3D, 4D – two-dimensional, three-dimensional, four-dimensional.

Introduction

Multi-dimensional NMR experiments have resulted in a major break-through in biology and chemistry including the determination of the chemical structure of small molecules and three-dimensional structure determination of proteins (Ernst et al., 1985). The underlying idea in two-dimensional time-domain spectroscopy is the use of two independent precession periods, during which coherence can evolve. However, coherence is observed only in the detection period. In the so-called indirect dimension, free chemical shift evolution is monitored indirectly by gradually increasing the evolution time (Wider, 1998). This concept was successfully extented from two-dimensional (Ernst et al., 1985) to three-dimensional experiments (3D; Oschkinat et al., 1989), and eventually three-dimensional triple-resonance experiments correlating three or more nuclei were developed (Grzesiek and Bax, 1993). However, the extension to four dimensions (4D) is only beneficial for a small number of experiments, i.e., 4D ^{13}C- and/or ^{15}N-resolved [^{1}H,^{1}H]-NOESY experiments (Kay et al., 1990a) and the 4D TROSY-HNCACO and HNCOCA experiments applied for deuterated proteins (Yang and Kay, 1999; Tugarinov et al., 2002). The major reasons why the number of dimensions cannot be increased to four or more are (i) the sensitivity loss of $\sqrt{2}$ per additional dimension due to the additional quadrature

*To whom correspondence should be addressed. E-mail: riek@sbl.salk.edu

detection needed, (ii) extensive signal losses due to relaxation during additional polarization transfer periods and evolution periods, and (iii) low resolution due to limited measuring time (Wider, 1998). The concept of reduced-dimensionality, which combines information from different evolution periods into one dimension incrementing two evolution times simultaneously and reducing the number of dimensions by one, offers a solution to the problem of low chemical shift resolution in 4D experiments (Szperski et al., 1993). However, reduced dimensionality experiments still suffer from extensive signal losses due to additional polarization transfer periods and evolution periods (Sattler et al., 1999).

In this paper, we introduce an alternative concept of monitoring chemical shifts in a multi-dimensional NMR experiment, in which a chemical shift can be added to an experiment without an additional chemical shift evolution and polarization transfers. The additional chemical shift is coded in the line-shape of a cross-peak through an apparent scalar coupling active during an established evolution period. The size of this scalar coupling is manipulated with an off-resonance radio-frequency pulse in order to correlate its size with the position of the additional chemical shift of interest. The proposed concept of coding chemical shift information in a residual scalar coupling might remind the reader of off-resonance decoupling, which was used extensively in the pre-multidimensional NMR history (Ernst, 1966; Tanabe et al., 1970) and for one specific problem in a multi-dimensional experiment (Fesik et al., 1990). However, as it will be pointed out in this work, the two methods are different.

We applied the proposed concept of chemical shift monitoring to the three-dimensional triple-resonance experiment HNCA (Kay et al., 1990b), which resulted in additional information of the $^1H^\alpha$ chemical shift. The experiment is called HNCA^{coded}HA, since the chemical shift of $^1H^\alpha$ is coded in the line-shape of the cross-peak through the scalar coupling $^1J(^{13}C^\alpha,^1H^\alpha)$.

Theory

We are considering a system of two scalar coupled spins 1/2, I and S, with a scalar coupling constant $^1J(I,S)$ located in a molecule. During the frequency labeling time t the chemical shift of spin S and the scalar coupling $^1J(I,S)$ are evolving, which results in a density matrix σ at time t (only terms of interest are listed):

$$\sigma[t] = S_x \cos[\omega_S t] \cos[\pi\ {}^1J(I,S)t] + \dots , \quad (1)$$

where ω_S is the Larmor frequency of spin S. With a 180° radio-frequency hard-pulse applied on spin I placed at time point $t/2$ the scalar coupling will be refocused according to the following formula:

$$\sigma[t] = S_x \cos[\omega_S t] + \dots . \quad (2)$$

Coding chemical shift information through the scalar coupling is based on the use of a 180° radio-frequency soft pulse applied on I at time point $t/2$. This soft pulse is set on-resonance at the high-field edge of the chemical shift range for spin I, designated with the Larmor frequency $\omega_{I,\max}$. The inversion profile $a(\omega_I)$ of this soft pulse is constructed in such a way that all the longitudinal magnetization at frequency $\omega_{I,\max}$ is completely inverted and the inversion decreases towards zero at $\omega_{I,\min}$, which designates the Larmor frequency of the low-field edge of the chemical shift range of spin I. Thus, the shoulder of the inversion profile of the soft pulse must cover the chemical shift range of all the spins I of the molecule. With the addition of such a soft pulse the scalar coupling $^1J(I,S)$ is refocused at time t for only some spins S ($a(\omega_I)$ * Equation 2 = second term in Equation 3) and is not refocused for the rest of the spins ($(1 - a(\omega_I))$ * Equation 1 = first term of Equation 3) yielding the following density matrix:

$$\begin{aligned}\sigma[t] \ = \ & S_x(1 - a(\omega_I)) \cos[\omega_S t] \cos[\pi\ {}^1J(I,S)t] + \\ & S_x a(\omega_I) \cos[\omega_S t] + \dots \end{aligned} \quad (3)$$

with $0 = a(\omega_{I,\min}) \leq a(\omega_I) \leq 1 = a(\omega_{I,\max})$. One would expect that in the transformed spectrum this mixed coherence will appear as a superposition of a doublet with frequencies $\omega_S + \pi\ {}^1J(I,S)$ and $\omega_S - \pi\ {}^1J(I,S)$ and a singlet with frequency ω_S and that the relative amplitude of the three components will depend on $a(\omega_I)$ (Figure 2B). However, with a $t_{\max}$ up to $\sim 1/{}^1J(I,S)$ the spectral resolution is too low for the observation of three multiplet components. In contrast, this mixed coherence appears as a doublet consisting of an apparent residual scalar coupling $^{residual}J(I,S)$, the size of which depends on $a(\omega_I)$ (Figure 2A):

$$\sigma[t] = S_x \cos[\omega_S t] \cos[\pi\ {}^{residual}J(I,S)t]. \quad (4)$$

As can be extracted from Figure 2A the apparent residual scalar coupling $^{residual}J(I,S) \approx (1 - a(\omega_I))$

$^1J(I,S)$. For simplicity, we use in the following this relationship and the assumption that the inversion profile of the applied softpulse $a(\omega_I)$ decays linearly from the value 1 at $\omega_{I,\max}$ to 0 inversion at $\omega_{I,\min}$. Under these assumptions, the following apparent residual scalar coupling is monitored:

$$^{\text{residual}}J(I,S) \approx \frac{\omega_{I,\max} - \omega_I}{\omega_{I,\max} - \omega_{I,\min}}\ ^1J(I,S). \quad (5)$$

In other words, the density matrix σ after time t is:

$$\sigma[t] \approx \quad (6)$$

$$S_x \cos[\omega_S t] \cos\left[\pi \frac{\omega_{I,\max} - \omega_I}{\omega_{I,\max} - \omega_{I,\min}}\ ^1J(I,S)t\right] + \ldots .$$

With Equation 6 it is evident that the Larmor frequency of spin I, ω_I, is monitored with the proposed concept. Furthermore, Equation 6 demonstrates that the accuracy of the determination of the chemical shift of spin I is proportional to the scalar coupling $^1J(I,S)$ and to the maximal evolution time $t_{\max}$, and inversely proportional to the chemical shift range of spin I, $\omega_{I,\max} - \omega_{I,\min}$. Thus, the chemical shift resolution is high with a large scalar coupling and a small chemical shift range. Interestingly, since $\omega_{I,\max} - \omega_{I,\min}$ and $\omega_{I,\max} - \omega_I$, are proportional to the external magnetic field *Bo*, the chemical shift resolution (in Hz) of the proposed concept is independent of the magnetic field *Bo*, in contrast to the resolution in the direct dimension, which increases with the magnetic field. Equation 6 illustrates furthermore the basic idea of the proposed technique: chemical shift-coding can be applied during any evolution periods, if a $^1J(I,S)$ with an appropriate size is present. And the technique could be applied several times within one evolution time or within one experiment, increasing further the number of monitored frequencies. The origin of the associated peak intensity loss is the cosine modulation of the residual scalar coupling (Equation 6), which results in a multiplet splitting of the cross-peak and thus may cause a signal intensity decrease of up to a factor of ∼2 (with an average signal intensity loss of 1.5). There is no additional signal loss due to transverse relaxation, since no polarization transfer periods and evolution periods have been introduced to monitor the additional chemical shifts. In contrast, due to active cross-correlated relaxation between $S - I$ dipole-dipole coupling and chemical shift anisotropy of spin S for those spins S, which are not refocused with the inversion profile $a(\omega_I)$ (first term of Equation 3), the proposed concept may profit in signal-to-noise from transverse relaxation-optimization (Pervushin et al., 1997; Riek et al., 2000) during evolution time t. But, since this effect results in a differential relaxation of the multiplet components, cross-correlated relaxation might affect the relationship between apparent residual scalar coupling and chemical shift. We calculated, that the influence of transverse relaxation T2 to the relationship between apparent residual scalar coupling and chemical shift can be neglected. For T2 = $1/^1J(I,S)$ and a cross-correlated relaxation rate of 2/(3 T2) the expected overestimation of the apparent residual scalar coupling is about 5% and thus within the accuracy of the method (data not shown).

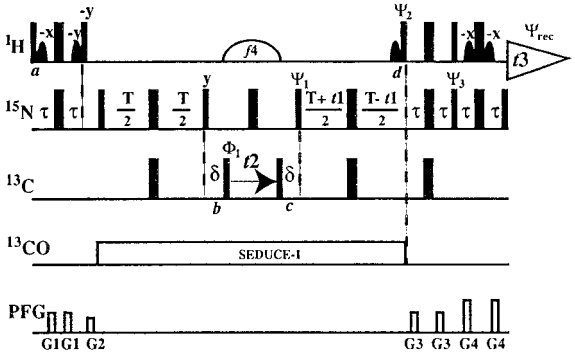

Figure 1. Experimental scheme for the HNCA$^{\text{coded}}$HA experiment for ^{13}C,^{15}N-labeled proteins. The radio-frequency pulses on ^{1}H, ^{15}N, $^{13}C^{\alpha}$ or $^{13}C'$ were applied at 4.8, 119, 55, and 174 ppm, respectively. The narrow and wide black bars indicate non-selective 90° and 180° pulses, respectively. On the line marked ^{1}H, black sine bell shapes indicate selective 90° pulses with the duration of 1 ms and a Gaussian shape truncated at 5% are applied on the water resonance. On the same line a large sine bell shaped pulse labeled with $f4$ indicates a selective 180° pulse with a Gaussian shape truncated at 5% and the duration of 1.3 ms. The soft pulse is on resonance at 3.5 ppm and its length has been optimized for the magnetic field strength of 700 MHz ^{1}H frequency. The inversion profile is shown in Figure 3A. The line marked PFG indicates durations and amplitudes of sine shaped pulse magnetic field gradients applied along the z-axis.: G1: 0.8 ms, 15 G cm^{-1}, G2: 0.8 ms, 9 G cm^{-1}; G3: 0.8 ms, 22 G cm^{-1}; G4: 0.8 ms, 22 G cm^{-1}. The delays τ, T, and δ are 2.7 ms, 24 ms and 1.3 × 0.5 ms, respectively. The phase cycle is $\Psi_1 = \{y,-y,x,-x\}$, $\Psi_2 = \{-y\}$, $\Psi_3 = \{-y\}$, $\Phi_1 = \{x, x, x, x,-x,-x,-x,-x\}$ and $\Phi_{\text{rec}} = \{y,-y,-x,x,-y,y,x,-x\}$. All other radio frequency pulses are applied either with phase x or as indicated above the pulses. In the ^{15}N($t1$) dimension a phase-sensitive spectrum is obtained by recording a second FID for each increment of $t1$, with $\Psi_1 = \{y, -y, -x, x\}$, $\Psi_2 = \{y\}$, $\Psi_3 = \{y\}$ and the data are processed as described by Kay et al. (1992). Quadrature detection in the $^{13}C^{\alpha}$ ($t2$) dimension is achieved by the States-TPPI method (Marion et al., 1989) applied to phase Φ_1. The water magnetization stays aligned along the $+z$-axis throughout the experiment by the use of water flip-back pulses (black sine bell shapes; Grzesiek and Bax, 1993). Between time points b and c the timing of the radio frequencies pulses of the different nuclei have been implemented in a parallel manner to achieve an initial $t_2 = 0$.

In an experiment, the applied soft pulse will not have a linear inversion profile as assumed above in Equations 5 and 6, but the inversion profile of the applied soft pulse will cover in a predictable way the chemical shift range. For example, the soft pulse used in the pulse sequence of Figure 1 contains a Gaussian shape with a truncation threshold C of 5% characterized by the following inversion profile (Hull, 1994):

$$a(\omega_I) = \exp[-(\omega_{I,\max} - \omega_I)^2 \ln(100/C)/(0.5(\omega_{I,\max} - \omega_{I,\min}))^2]. \quad (7)$$

Furthermore, for a precise evaluation of the chemical shift of spin I, Equation 3 instead of Equation 4 should be used.

Alternatively, off-resonance decoupling with a resonance frequency of ω_{cw} and a radio-frequency power of $\gamma_H B_2/2\pi$ can be used to scale the scalar coupling $^1J(I,S)$ depending on the chemical shift of spin I (Ernst, 1966; Tanabe et al., 1970; Freeman, 1988). The observed scaled scalar coupling is a *real* residual scalar coupling, since the off-resonance irradiation on spin I is applied during the entire period t and thus affects the effective magnetic field of spin S (for more details see Ernst, 1966; Tanabe et al., 1970; Freeman, 1988). Provided that $\omega_{cw} - \omega_I$ is large compared with $0.5\ ^1J(I,S)$ and the decoupling time t is long, the following residual splitting is expected (Freeman, 1988):

$$^{\text{residual}}J(I,S) \approx (\omega_{cw} - \omega_I)/([\omega_{cw} - \omega_I]^2 + (\gamma_H B_2/2\pi)^2]^{0.5})\ ^1J(I,S). \quad (8)$$

A comparison between the two discussed concepts yields the following observations: (i) The residual scalar coupling $^{\text{residual}}J(I,S)$ derived from off-resonance decoupling (Equation 8) is a *real* residual scalar coupling (Freeman, 1988), which is in contrast to the apparent residual scalar coupling derived from chemical shift-coding (Equations 3 and 5, Figure 2). (ii) The relationships between the residual scalar couplings and the chemical shifts of interest are strongly dependent on the chosen concept, as can be depicted from Figures 3A and B and Equations 7 and 8. (iii) The concept of chemical shift-coding was developed for times t with $0 < t < 1/^1J(I,S)$ and can therefore be optimally incorporated in any evolution times during an experiment (see below), whereas off-resonance decoupling is only well suited for $t \gg 1/^1J(I,S)$ and is thus preferably applied during acquisition (Freeman, 1988; Fesik et al., 1990; Ernst, 1966).

Methods

The concept of chemical shift-coding introduced above was applied to the 3D HNCA experiment adding the chemical shift of $^1H^\alpha$. The so-called HNCA$^{\text{coded}}$HA experiment is based on the TROSY (Pervushin et al., 1997) version of the HNCA experiment (Salzmann et al., 1999) with only one minor but pivotal difference during the alpha-carbon evolution depicted in Figure 1, which shows the experimental scheme for the HNCA$^{\text{coded}}$HA experiment. Between time points a and b, magnetization is transferred from ^1H via ^{15}N to $^{13}C^\alpha$, using two successive INEPT steps (Morris and Freeman, 1979). During the frequency labeling period t_2 the $^{13}C^\alpha$ chemical shift evolves. Simultaneously, the $^1J(^{13}C^\alpha,^1H^\alpha)$ scalar coupling of ~144 Hz begins to evolve. However, the apparent extent of the evolution of the $^1J(^{13}C^\alpha,H^\alpha)$ coupling is under the control of the 180° soft pulse on $^1H^\alpha$. The soft pulse is on-resonance at the high-field edge of the $^1H^\alpha$ chemical shift range at 3.5 ppm and contains a Gaussian inversion profile, which decreases to ~5% at 5.0 ppm (Figure 3A). Thus, the multiplet splitting of the cross-peak along the $^{13}C^\alpha$ dimension and the concomitant apparent extent of the $^1J(^{13}C^\alpha,1H^\alpha)$ coupling depend on the position of the attached $^1H^\alpha$ chemical shift (Figure 3A). In other words, the $^1H^\alpha$ chemical shift is encoded in the pattern of the cross-peak along ^{13}C dimension through an apparent residual scalar coupling $^{\text{residual}}J(^{13}C^\alpha,^1H^\alpha)$ (Figure 3A; Equations 3, 4 and 7). A theoretical description of the concept was given in the theory section. After chemical shift evolution modulated by the chemical shift-dependent scalar coupling, magnetization is transferred back to ^{15}N at time point c. Between c and d the ^{15}N nuclei evolve with their chemical shifts during a constant time period. From time point d onward magnetization is transferred back to ^1H. The coherence flow can thus be described as follows:

$$^1H(i) \rightarrow {}^1H(i) \begin{matrix} \nearrow {}^{13}C^\alpha(i)[t2]\cos[\pi\,{}^{\text{residual}}J(^{13}C^\alpha(i),{}^1H^\alpha(i))t2] \\ \searrow {}^{13}C^\alpha(i-1)[t2]\cos[\pi\,{}^{\text{residual}}J(^{13}C^\alpha(i-1),{}^1H^\alpha(i-1))t2] \end{matrix} \nearrow$$
$$^1H(i)[t3] \rightarrow {}^1H(i)[t3],$$

where $t1$ and $t2$ are the ^{15}N and ^{13}C evolution times and $t3$ is the ^1H acquisition time. Indices i and $i-1$ indicate that coherence is transferred from $^{15}N(i) - {}^1H(i)$ to both the sequentially and the intra-residually adjoining $^{13}C^\alpha$'s, respectively. The coded $^1H^\alpha$ chemical shift is designated with the cosine modulation of its apparent residual scalar

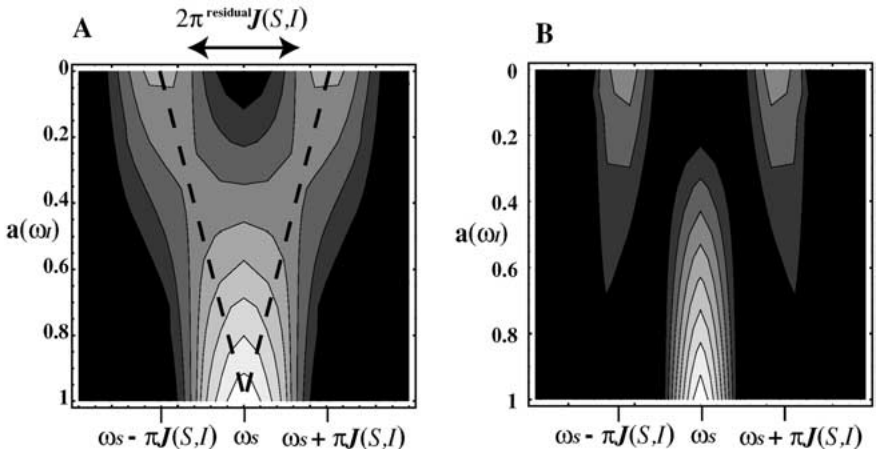

Figure 2. Contourplots of the relationship between the inversion profile $a(\omega_I)$ of the soft pulse and the peak shape in the transformed spectrum along frequency ω_S with (A) a $t_{max} = 1\ ^1J(S,I)$ and (B) a $t_{max} = 2\ ^1J(S,I)$. A comparison of the two contourplots shows that the introduction of apparent residual scalar coupling $^{residual}J\ (S,I) = (1 - a(\omega_I))\ ^1J(S,I)$ is only appropriate for maximal evolution times t_{max} up to $\sim 1\ ^1J(S,I)$. In (A) the relationship $^{residual}J\ (S,I) = (1 - a(\omega_I))\ ^1J(S,I)$ is shown by dashed lines: For $a(\omega_I = \omega_{max}) = 1\ ^{residual}J\ (S,I) = {}^1J(S,I)$ is observed, and for $a(\omega_I = \omega_{min}) = 0$ a $^{residual}J\ (S,I) = 0$ is observed. The contourplots were generated by Fourier transformation of Equation 3. Darker contours indicate lower intensities.

coupling, $^{residual}J(^{13}C^{\alpha},{}^1H^{\alpha})$, active during $t2$. The relationship between the $^1H^{\alpha}$ chemical shift and $^{residual}J(^{13}C^{\alpha},{}^1H^{\alpha})$ depends on the inversion profile of the soft pulse used. In the experiment presented in Figure 1 a soft pulse with a Gaussian inversion profile and the length of 1.3 ms on-resonance at 3.5 ppm was applied. The corresponding relationship between $^{residual}J(^{13}C^{\alpha},{}^1H^{\alpha})$, and the chemical shift is given in Figure 3A.

Results and discussion

The relation between $^{residual}J(^{13}C^{\alpha},\ ^1H^{\alpha})$ and $^1H^{\alpha}$ chemical shift

As described in the theory section (Equations 3–6), the proposed concept of chemical shift-coding is based on a specific relation between an apparent residual scalar coupling and the chemical shift of interest, which is a function of the inversion profile of the chosen soft pulse. Since we are using a soft pulse with a Gaussian inversion profile, the correlation of the apparent residual scalar coupling with the chemical shift of interest is theoretically also approximately a Gaussian function (Equation 7 and Figure 3A). To verify the calculated function, the expected relationship was measured experimentally using a test sample containing 10 mM ^{13}C,^{15}N-labeled leucine. In an array of one-dimensional ^{13}C-^1H correlation experiments a selective $^1H^{\alpha}$ filter with the soft pulse of interest was applied upon magnetization transfer from ^1H to ^{13}C, followed by back-transfer to ^1H and acquisition (see also caption to Figure 3). In this array, the resonance frequency of the Gaussian soft pulse with length 1.3 ms was incremented in steps of 100 Hz with a starting ^1H-frequency that corresponds to the $^1H^{\alpha}$ chemical shift of leucine. The off-resonance inversion effects of the Gaussian soft pulse onto the measured $^1H^{\alpha}$ signal are displayed in Figure 3A and show a perfect match between the measured data points and the calculated relationship. We further evaluated the influence of radio frequency imperfections on the relationship between the apparent residual scalar couplings and the corresponding chemical shifts. The same array of one-dimensional experiments was acquired, this time, however, with a radio frequency power of the Gaussian soft pulse off-calibrated by 10% (10% less power than optimal). As can be inferred from Figure 3A, the off-calibration of the radio frequency power of the soft pulse influences the relationship between the apparent residual scalar coupling and the chemical shift only when the chemical shift is close to the resonance frequency of the soft pulse. Therefore, it can be concluded that the calculated relationship between the apparent residual scalar coupling and the chemical shift is experimentally established in a reliable way.

As mentioned in the Theory section, the relationship between a $^{residual}J(^{13}C^{\alpha},{}^1H^{\alpha})$ and a $^1H^{\alpha}$ chemical shift can also be established using off-resonance decoupling. To verify the relationship given in Equa-

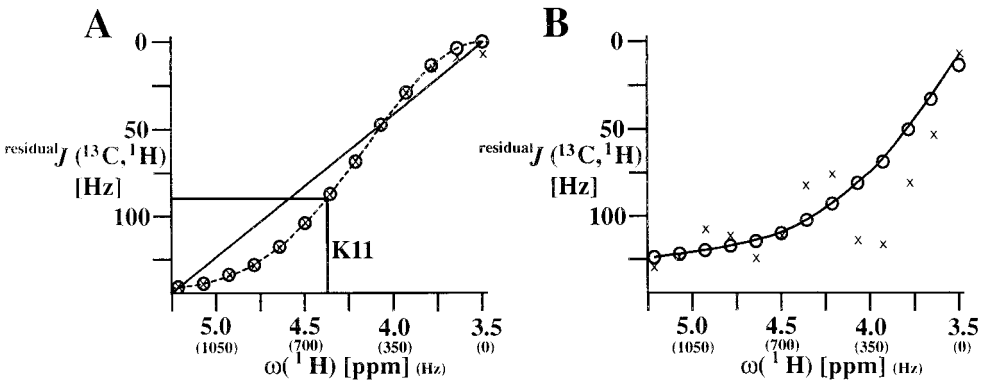

Figure 3. The relationship between the $^1H^\alpha$ chemical shift and the apparent residual scalar coupling $^{residual}J(^{13}C^\alpha,^1H^\alpha)$ applying (A) a off-resonance softpulse and (B) off-resonance cw decoupling. (A) The continous line was plotted on the basis of Equation (5) assuming a proportional relation between the $^1H^\alpha$ chemical shift and the corresponding $^{residual}J(^{13}C^\alpha,^1H^\alpha)$. For the calculation $\omega_{I,max} = 3.5$ ppm and $\omega_{I,min} = 5.3$ ppm were used. The dashed curve represents the relationship between the chemical shift and the apparent residual scalar coupling established by the Gaussian soft pulse with the length of 1.3 ms used in the HNCA^{coded}HA experiment (see caption to Figure 1). The relationship shown corresponds to the inversion profile of the soft pulse. The $^1H^\alpha$ chemical shifts in Figures 3, 4 and 5 have been extracted from the dashed plot as shown for residue 11 upon the measurement of the apparent residual scalar coupling (see Figure 5). The relationship measured experimentally with a proper calibration of the soft-pulse is marked with circles; the relationship measured with a 10% off-calibrated radio-frequency power of the soft-pulse is marked with crosses. The experimentally measured relationship was acquired with $^{13}C,^{15}N$-labeled Leu in an array of one-dimensional ^{13}C-^1H correlation experiments including a selective $^1H^\alpha$ filter: $\pi/2(^1H) - 1/4J(^1H,^{13}C) - \pi(^1H),\pi(^{13}C) - 1/4J(^1H,^{13}C) - \pi/2(^1H),\pi/2(^{13}C) - 1/4J\ (^1H,^{13}C) - \pi$-softpulse$(^1H),\pi(^{13}C) - 1/4J(^1H,^{13}C) - \pi/2(^1H),\pi/2(^{13}C) - 1/4J(^1H,^{13}C) - \pi(^1H),\pi(^{13}C) - 1/4J(^1H,^{13}C)$. In this array, the resonance frequency of the Gaussian soft pulse with length 1.3 ms was incremented in steps of 100 Hz with a starting ^1H-frequency that corresponds to the $^1H^\alpha$ chemical shift of leucine. The off-resonance inversion effects of the Gaussian soft pulse onto the measured $^1H^\alpha$ signal show a perfect match between the measured data points and the calculated relation. In brackets, the relative difference between the resonance frequency of the Gaussian soft-pulse or the decoupling frequency and the $^1H^\alpha$ chemical shift of $^{13}C,^{15}N$-labeled Leu are given in Hz.

(B) The continous line represents the calculated relationship between the chemical shift and the residual scalar coupling established by cw decoupling at $\omega_{cw} = 3.5$ ppm (0 Hz) with radio-frequency power $\gamma_H\ B_2/2\pi$ of 600 Hz. The calculated relationship of interest was plotted on the basis of equation [8] assuming an infinite time t. The relationship measured experimentally with an off-resonance decoupling time $\tau = 1/[2^1J(S,I)] = 3.4$ ms is marked with crosses; the relationship measured with an off-resonance decoupling time $\tau = 15/[2^1J(S,I)] = 51$ ms is marked with circles. The experimentally measured relationship was acquired with $^{13}C,^{15}N$-labeled Leu in an array of one-dimensional ^{13}C-^1H correlation experiments including off-resonance decopuling: $\pi/2(^1H) - 1/4J(^1H,^{13}C) - \pi(^1H),\pi(^{13}C) - 1/4J(^1H,^{13}C) - \pi/2(^1H),\pi/2(^{13}C) - \tau - \pi(^{13}C) - \tau - \pi/2(^1H),\pi/2(^{13}C) - 1/4J(^1H,^{13}C) - \pi(^1H),\pi(^{13}C) - 1/4J(^1H,^{13}C)$. In this array, the resonance frequency of the off-resonance decoupling during the time $2 \times \tau$ was incremented in steps of 100 Hz with a starting ^1H-frequency that corresponds to the $^1H^\alpha$ chemical shift of leucine.

tion 8, an array of one-dimensional ^{13}C-^1H correlation experiments was measured with a set-up similar to the one used above, but the Gaussian soft-pulse was replaced by off-resonance decoupling with a radio frequency power $\gamma_H\ B_2/2\pi$ of 600 Hz applied during the entire filtering element with length t. The measured function of the residual scalar coupling *versus* the offset between the $^1H^\alpha$ chemical shift and decoupling frequency ω_{cw} is displayed in Figure 3B. With a filtering element length t of $1/(2^1J(^{13}C^\alpha,^1H^\alpha)) = 3.4$ ms the inversion profile of off-resonance decoupling performs oscillatory and does not match the calculated relationship (Figure 3B). Only with very long off-resonance decoupling times ($t = 50$ ms) the predicted relationship between residual scalar coupling and $^1H^\alpha$ chemical shift was realized. This finding makes clear that off-resonance decoupling should not be used during indirect dimensions of NMR experiments starting with an evolution time $t = 0$. On the other hand, off-resonance decoupling can be applied during acquisition, for example to correlate ^1H and ^{13}C chemical shifts of small molecules (Ernst et al., 1985; Tanabe et al., 1970) or to determine ^{15}N chemical shifts of NOEs between amide hydrogens and aliphatic hydrogens in a 3D ^{13}C-resolved $[^1H,^1H]$-NOESY experiment (Fesik et al., 1990).

3D HNCA^{coded} HA experiment: An application of the concept of chemical shift-coding

Figure 4A shows strips and cross-sections from a 3D HNCA^{coded}HA spectrum of uniformly $^{13}C,^{15}N$-labeled ubiquitin. As in the conventional HNCA experiment (Figure 4B), two cross-peaks are observed

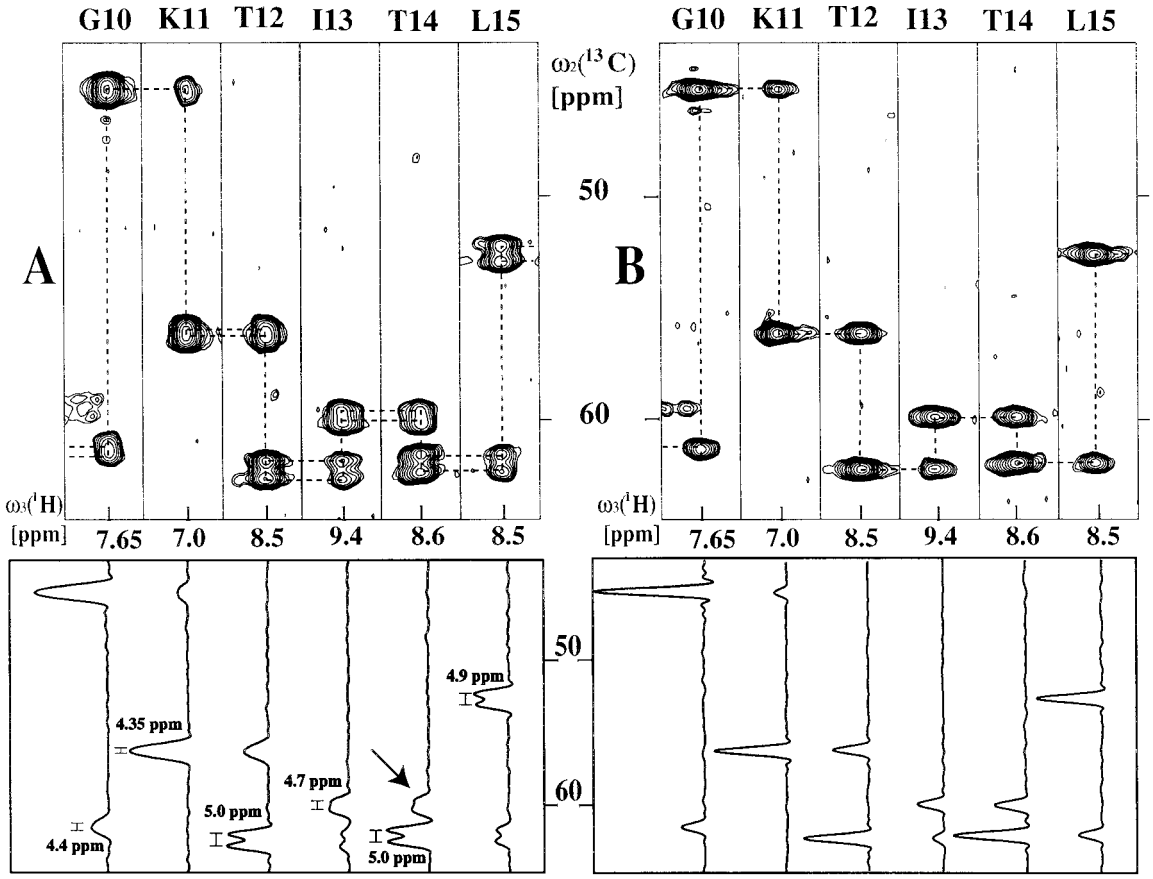

Figure 4. (A) Strips and corresponding cross-sections along the $\omega_2(^{13}C)$ dimension of the 3D HNCA^{coded}HA spectrum of $^{13}C,^{15}N$-labeled ubiquitin. (B) Analogous strips and corresponding cross-sections of the HNCA spectrum. The strips are centered about the corresponding $^1H^N$ chemical shifts. At the top the sequence-specific assignments are indicated by the one-letter amino acid code and by the sequence number. The sequential connectivities are indicated by horizonal dashed lines. The $^1H^\alpha$ chemical shifts have been extracted from the dashed plot in Figure 3A upon the measurement of the apparent residual scalar coupling with a modified version of the program INFIT (Szyperski et al., 1992). Designated by an arrow is a characteristic multiplet, for which the multiplet components have different intensities due to cross-correlated relaxation between $^{13}C^\alpha$–$^1H^\alpha$ dipole-dipole coupling and alpha-carbon chemical shift anisotropy. The experiments were recorded at 20 °C with a 0.8 mM sample of $^{13}C,^{15}N$-labeled ubiquitin in a mixed solvent of 95% H_2O/5% D_2O at pH 7, using a Bruker Avance 700 MHz spectrometer equipped with five radio-frequency channels, a pulsed field gradient unit and a triple resonance probe with an actively shielded z-gradient coil. The following parameter settings were used for both experiments: data size = 50($t1$)×50($t2$)×1024($t3$) complex points; $t1_{max}$ (^{15}N) = 24 ms, $t2_{max}$ ($^{13}C^\alpha$) = 8.7 ms, $t3_{max}$(^1H) = 75.6 ms. The data set was zero-filled to 128×512×2048 complex points; 8 scans per increment were acquired, resulting in 17 h of measuring time. Prior to Fourier transformation the data were multiplied with a 75° shifted sine bell window in all dimensions.

for each spin system: The stronger cross-peak corresponds to intra-residue correlations between the carbons and the ^{15}N-^1H moiety, and the weaker cross-peak represents the sequential correlations. In addition, these cross-peaks are split due to the active $^{residual}J(^{13}C^\alpha,^1H^\alpha)$-coupling, the size of which is related to the $^1H^\alpha$ chemical shift as depicted in Figure 3A: The cross-peak is not split if the attached $^1H^\alpha$ chemical shift is 3.5 ppm, the cross-peak is a doublet of 144 Hz if the corresponding $^1H^\alpha$ chemical shift is $\geq$ 5.3 ppm, and an apparent residual scalar coupling of 0–144 Hz corresponds to a $^1H^\alpha$ chemical shift between 3.5–5.3 ppm (Figures 3 and 4A). The sizes of the apparent residual scalar couplings were evaluated with a modified version of the program INFIT (see caption to Figure 5 and Szyperski et al., 1992) and the corresponding $^1H^\alpha$ chemical shifts were extracted using Equation 7 (see also Figure 3A). In Figure 5 the $^1H^\alpha$ chemical shifts extracted from the proposed technique of chemical shift-coding were plotted versus their values measured with the conventional technique to exploit their experimen-

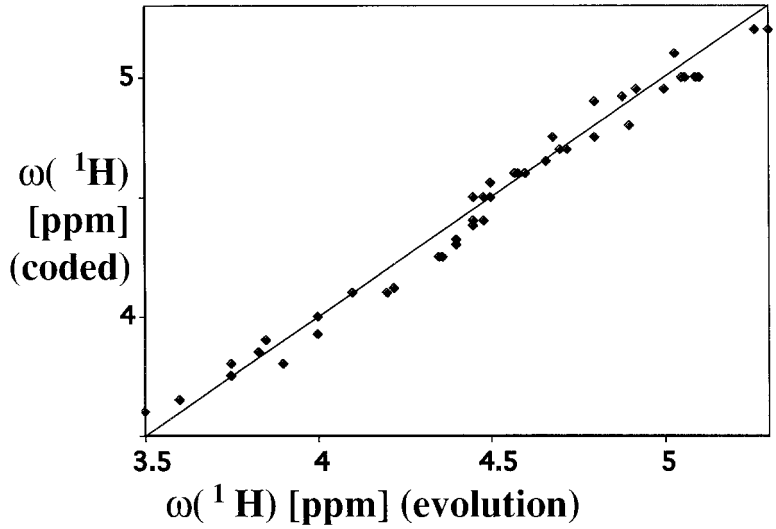

Figure 5. $^{1}H^{\alpha}$ chemical shifts of ^{13}C,^{15}N-labeled ubiquitin derived from the HNCA^{coded}HA experiment plotted *versus* the chemical shifts measured by chemical shift evolution (for measuring conditions see Figure 4). Using Equation 7 the chemical shifts were calculated from the extracted apparent residual scalar coupling. The apparent residual scalar coupling were obtained with a modified version of the software INFIT (Szyperski et al., 1992), which determines scalar couplings by inverse Fourier transformation of in-phase multiplets. INFIT takes into account the limited digitization, the T2 relaxation, and the window function used. The modified version considers also the active scalar coupling $^{1}J(^{13}C^{\alpha},^{13}C^{\beta}) = 35$ Hz. The presence of two chemical shifts per glycine residue makes the extrapolation of the chemical shifts from the apparent residual scalar coupling more demanding. Thus, the chemical shifts of glycines have been excluded from the plot.

tal accuracy. The observed excellent correlation of the determined chemical shifts strongly supports the concept of chemical shift-coding. The accuracy of the determination of the $^{1}H^{\alpha}$ chemical shifts in the HNCA^{coded}HA experiment is mainly limited by the maximal evolution time of carbons, $t2_{max}$, the size of the scalar coupling $^{1}J(^{13}C^{\alpha},^{1}H^{\alpha})$, and the spectral range of the $^{1}H^{\alpha}$ chemical shifts, which has to be covered by the shoulder of the inversion profile of the soft-pulse (Equations 3, 4 and 7; see the Theory section). Using a $^{1}J(^{13}C^{\alpha},^{1}H^{\alpha})$ coupling of ~144 Hz, a $^{1}H^{\alpha}$ spectral range of 1.8 ppm, a magnetic field strength of 700 MHz ^{1}H frequency and assuming that the $^{residual}J(^{13}C^{\alpha},^{1}H^{\alpha})$-coupling can be evaluated with a precision of 8 Hz, it can be calculated from Equation 5 that the accuracy of the determined $^{1}H^{\alpha}$-chemical shifts is ~70 Hz, which coincides well with the experimentally obtained accuracy (Figure 5). In this evaluation the glycine residues were excluded, since the presence of two alpha-hydrogen $^{1}H^{\alpha}$ per $^{13}C^{\alpha}$ makes the extrapolation of two $^{1}H^{\alpha}$ chemical shifts from one apparent residual scalar coupling more demanding (but see below). Thus, with the introduction of one simple soft pulse during the carbon evolution in the 3D HNCA experiment, the $^{1}H^{\alpha}$-chemical shifts can be determined in addition to the $^{1}H^{N}$, ^{15}N and $^{13}C^{\alpha}$ chemical shifts.

Moreover, with the introduction of one simple soft pulse the quality of correlation of sequential residues improved dramatically, because the sequential correlation in the 3D HNCA^{coded}HA experiment can be traced on the basis of $^{13}C^{\alpha}$ and $^{1}H^{\alpha}$ chemical shifts; in the conventional 3D HNCA experiment the sequential residues are traced only by the $^{13}C^{\alpha}$ chemical shifts. Using a $^{1}H^{\alpha}$ chemical shift accuracy of 0.1 ppm (see above) and a $^{1}H^{\alpha}$ chemical shift dispersion of 1.8 ppm, it can be therefore estimated that the additional information of the $^{1}H^{\alpha}$ chemical shift increases the quality of a sequential correlation by a factor of ~18. Indeed, with the HNCA^{coded}HA experiment a straight-forward sequential walk can be traced through the multiplets of the $^{13}C^{\alpha}$ cross-peak including the overall position of the $^{13}C^{\alpha}$ cross-peak as a point of departure (see Figure 4). When a multiplet pattern of a sequential cross-peak coincides with a multiplet of an intra-residual cross-peak, the sequential connectivity is traced and ensured by two independent correlations, the alpha-carbon and alpha-hydrogen chemical shifts. When the patterns do not fit, the two involved ^{15}N-^{1}H moieties are not neighbors. Importantly, the proposed procedure for tracing sequential correlations profits from the $^{1}H^{\alpha}$ chemical shifts through the apparent residual scalar coupling and therefore without explicit extraction of the chemical shifts. Thus, the $^{1}H^{\alpha}$ chemical shifts of

the glycine residues can also be used for the sequential assignment through the apparent residual scalar coupling, although the extrapolation of their chemical shifts is not straightforward (see above). In conclusion, the proposed procedure reduces dramatically ambiguities in linking the spin systems of adjacent residues in the protein sequence during the sequential assignment process.

The improvement of the quality of correlations through the introduction of chemical shift-coding is connected with a moderate peak intensity loss due to the splitting of the cross-peak. The volume of the cross-peak is, however, not affected by chemical shift-coding. Furthermore, since the origin of the signal loss is the splitting of the cross-peak due to the apparent residual scalar coupling and since no additional polarization transfers and evolution periods have been introduced to monitor the additional chemical shift, this peak intensity loss is independent of the size of the molecule. Thus, a signal-to-noise loss of a factor of 2 has to be anticipated if a cross-peak is split completely into a doublet and the maximal signal-to-noise loss of ~2.2 will be observed for a cross-peak with a residual scalar coupling $2/3 \times {}^1J({}^1\mathrm{H},{}^{13}\mathrm{C})$. However, since a lot of cross-peaks split only partially, the average signal-to-noise loss is ~1.5 without affecting the volume of the cross-peak, as illustrated with the cross-sections of the HNCA and of the HNCA$^{\mathrm{coded}}$HA experiments (Figure 4). For comparison, a corresponding 4D HNCAHA experiment would suffer from (i) a sensitivity loss of $\sqrt{2}$ for the additional ${}^1\mathrm{H}^{\alpha}$ dimension due to the additional quadrature detection needed, (ii) 14%, 25% or 43% signal loss for a molecule with a rotational correlation time of 4 ns, 8 ns, or 16 ns, respectively, due to ${}^{13}\mathrm{C}^{\alpha}$ transverse relaxation ($T2({}^{13}\mathrm{C}^{\alpha}) =$ 50 ms, 25 ms, 12.5 ms, respectively, Lee et al., 1997) occurring during the additional two polarization transfer elements from ${}^{13}\mathrm{C}^{\alpha}$ to ${}^1\mathrm{H}^{\alpha}$ and from ${}^1\mathrm{H}^{\alpha}$ to ${}^{13}\mathrm{C}^{\alpha}$, (iii) ~25% signal loss due to B_2 inhomogeneity of the additional 8 pulses of the additional polarization transfer elements, (iv) up to 15% signal loss due to a partial active ${}^1J({}^{13}\mathrm{C}^{\alpha}, {}^{13}\mathrm{C}^{\beta})$ coupling during the above mentioned polarization transfer elements, (v) additional signal loss due to $T2({}^1\mathrm{H}^{\alpha})$ relaxation and active ${}^1J({}^1\mathrm{H},{}^1\mathrm{H})$ couplings during the additional evolution period. The given numbers were calculated and confirmed experimentally for a rotational correlation time of 4 ns (data not shown).

Conclusion

The concept of coding a chemical shift through an apparent residual scalar coupling in the line-shape of a cross-peak of an adjoined nucleus has been demonstrated convincingly with the HNCA$^{\mathrm{coded}}$HA experiment. The strength of the concept is the addition of chemical shift information without any additional polarization transfers or/and evolution times resulting in a highly sensitive experiment with high quality information. Furthermore, the inherent basic idea of the technique and the ease of implementation open this technique to a wide range of multi-dimensional experiments despite the limitation of a $t_{\max} \leq 1/{}^1J(I,S)$. Indeed, preliminary data applying chemical shift coding to HNCACB$^{\mathrm{coded}}$HAHB (Pegan, Kwiatkowski, Choe, Riek, submitted) experiments and HNCA$^{\mathrm{coded}}$CB experiments are promising (C. Ritter, T. Luhrs, W. Kwiatkowski, R. Riek, in preparation).

It is our belief that this is an important technique for NMR-based structural genomics and for the study of structure-activity relationships by NMR, since one of the major challenges of these applications is optimal matching of instrument time with an appropriate information content (Montelione et al., 2000; Zuiderweg, 2002). The proposed concept of chemical shift-coding satifies both requirements.

Acknowledgements

We thank Dr Helena Kovacs for preliminary measurements and helpful discussions. We thank Dr Ad Bax for discussions and Dr Magda Kwiatkowski for careful reading. Furthermore, we thank the H. and J. Weinberg Foundation, the H.N. and F. C. Berger Foundation and the Auen Foundation for financial support.

References

Bax, A. and Grzesiek, S. (1993) *Acc. Chem. Res.*, **26**, 131–138.
Ernst, R.R. (1966) *J. Chem. Phys.*, **45**, 3845–3850.
Ernst, R.R., Bodenhausen, G. and Wokaun A. (1985) *Principles of Nuclear Magnetic Resonance in One and Two Dimensions*, Clarendon Press, Oxford.
Fesik, S.W., Eaton, H.L., Olejniczak, E.T. and Gampe, R.T. (1990) *J. Am. Chem. Soc.,* **112**, 5370–5371.
Freeman, R. (1988) *A Handbook of Nuclear Magnetic Resonance*, Longman Scientific & Technical, Essex.
Grzesiek, S. and Bax, A. (1993) *J. Am. Chem. Soc.,* **115**, 12593–12594.
Güntert, P., Dötsch, V., Wider, G. and Wüthrich, K. (1993) *J. Biomol. NMR*, **2**, 619–629.

Hull, W.E. (1994) In *Two Dimensional NMR Spectroscopy*, Croasmun, W.R. and Carlson, R.M.K. (Eds.), VCH, New York, NY.

Kay, L.E., Clore, G.M., Bax, A. and Gronenborn, A.M. (1990a) *Science*, **249**, 411–414.

Kay, L.E., Ikura, M., Tschudin, R. and Bax, A. (1990b). *J. Magn. Reson.*, **89**, 496–514.

Kay, L.E., Keifer, P. and Saarinen, T. (1992) *J. Am. Chem. Soc.*, **114**, 10663–10665.

Lee, L.K. Rance, M., Chazin, W.J. and Palmer, A.G. (1997). *J. Biomol. NMR*, **9**, 287–298.

Marion, D., Ikura, M., Tschudin, R. and Bax, A. (1989) *J. Magn. Reson.*, **85**, 393–399.

Montelione, G.T., Zheng, D., Huang, Y.J., Gunsalus, K.C. and Szyperski, T. (2000) *Nat. Struct. Biol.*, **7**, 982–985.

Morris, G.A. and Freeman, R. (1979) *J. Am. Chem. Soc.*, **101**, 760–762.

Oschkinat, H., Griesinger, C., Kraulis, P.J., Sorensen, O.W., Ernst, R.R., Gronenborn, A.M. and Clore, G.M. (1989) *Nature*, **332**, 374–376.

Pervushin, K., Riek, R., Wider, G. and Wüthrich, K. (1997) *Proc. Natl. Acad. Sci. USA*, **94**, 12366–12371.

Riek, R., Pervushin, K. and Wüthrich, K. (2000) *Trends Biochem. Sci.*, **25**, 462–468.

Salzmann, M., Pervushin, K., Wider, G., Senn, H. and Wüthrich, K. (1998) *Proc. Natl. Acad. Sci. USA*, **95**, 13585–13590.

Sattler, M., Schleucher, J. and Griesinger, C. (1999) *Prog. Nucl. Magn. Reson. Spectr.*, **34**, 93–158.

Szyperski, T., Guntert, P., Otting, G. and Wüthrich, K. (1992). *J. Magn. Reson.*, **99**, 552–560.

Szyperski, T., Wider, G., Bushweller, J. and Wüthrich, K. (1993) *J. Am. Chem. Soc.*, **115**, 9307–9308.

Tian, F., Valafar, H. and Prestegard, J.H. (2001) *J. Am. Chem. Soc.*, **123**, 11791–11796.

Tanabe, M, Hamasaki, T. and Thomas, T. (1971) *J. Am. Chem. Soc.*, **93**, 273–274.

Tugarinov, V., Muhandiram, R., Ayed, R. and Kay, L.E. (2002) *J. Am. Chem. Soc.*, on-line.

Wider, G. (1998) *Prog. NMR Spectr.*, **32**, 193–275.

Yang, D. and Kay, L.E. (1999) *J. Am. Chem. Soc.,* **121**, 2571–2575.

Zuiderweg, E.R. (2002) *Biochemistry*, **41**, 1–7.